(13) Parker, C. A. *Photoluminescence of Solutions*; Elsevier Publishing Co.: New York, 1968; p 92.
(14) This procedure was suggested to us by Professor L. T. Scott of this department to whom we express thanks.
(15) Burkhart, R. D.; Caldwell, N. J.; Haggquist, G. W. *J. Photochem. Photobiol., A, Chem.* **1988**, *152*, 56.
(16) Berlman, I. B. *Handbook of Fluorescence Spectra of Aromatic Molecules*; Academic Press: New York, 1965; p 108.
(17) *UV Atlas of Organic Compounds*; Plenum Press: New York; 1968; Vol. 4.
(18) Burkhart, R. D.; Aviles, R. G. *J. Phys. Chem.* **1979**, *83*, 1897.
(19) Caldwell, N. J.; Burkhart, R. D. *Macromolecules* **1986**, *19*, 1653.
(20) Richert, R.; Ries, B.; Bassler, H. *Philos. Magn. B* **1984**, *49*, L25.
(21) Johnston, L. J.; Scaiano, J. C.; Wilson, T. *J. Am. Chem. Soc.* **1987**, *109*, 1291.

Copolymerization of Hexafluoroisobutylene and Vinyl Acetate

Chengjiu Wu,* Raymond Brambilla, and James T. Yardley

Research and Technology, Allied-Signal, Inc., Morristown, New Jersey 07960.
Received November 14, 1988; Revised Manuscript Received August 9, 1989

ABSTRACT: Alternating copolymers of hexafluoroisobutylene (HFIB, monomer B) and vinyl acetate (VA, monomer A) were prepared under homogeneous radical conditions, and their structures were studied. The microstructure of the copolymers was studied by proton, carbon-13, and fluorine NMR. Monomer reactivity ratios were determined by a nonlinear least-squares procedure and from an analysis of the sequence distributions. The results support a penultimate model in which $r_{aa} = 0.0066$, $r_{ba} = 0.0405$, and $r_{bb} = r_{ab} = 0$. Configurational studies indicated that the stereochemistry of the alternating copolymers is not random and the tacticity is related to polymerization temperature. Bulk properties of the copolymers were examined by DSC, dielectric relaxation, and the XRD method. Alternating copolymers of HFIB and vinyl alcohol were also prepared.

Introduction

Although hexafluoroisobutylene (3,3,3-trifluoro-2-(trifluoromethyl)propene, referred to as HFIB or monomer B) and its copolymer with vinylidene fluoride (VDF) are now commercially available,[1] little is known about the polymerization behavior of HFIB and the microstructure of its copolymers. Infrared,[2] dielectric relaxation,[3] and X-ray diffraction[4] studies of the HFIB-VDF copolymer have been reported, indicating the crystalline and alternating nature of this copolymer. The scarcity of detailed NMR work on this copolymer is mainly due to its insolubility in solution.

NMR is a powerful tool for studying the microstructures of polymers.[5,6] For this purpose a soluble copolymer of HFIB is desirable. We report here the preparation of an amorphous and soluble copolymer of HFIB with a nonfluorinated vinyl monomer and a study of the microstructure of this copolymer. Vinyl acetate (referred to as VA or monomer A) was chosen since it readily copolymerizes with fluoroolefins[7] and since most of its copolymers, such as those with vinylidene cyanide (VDCN),[8] are amorphous.

Experimental Section

Hexafluoroisobutylene was obtained from Daikin Corp. and used without further purification. NMR spectra were obtained in $CDCl_3$ solution: ^1H (TMS standard, ppm) 6.33; ^{13}C (TMS standard, ppm) 130.3 (C_α, J_{C-F} = 33.5 Hz), 127.5 (C_β, J_{C-F} = 4.8 Hz), 120.4 (CF_3, J_{C-F} = 273 Hz); ^{19}F (C_6F_6 standard, ppm), −66.6. Vinyl acetate (Aldrich) was purified by fractional distillation. Azobis(isobutyronitrile) (AIBN, Aldrich) was recrystallized from ether. Vazo-33 (2,2-azobis(2,4-dimethyl-4-methoxyvaleronitrile)) was obtained from Du Pont and was used as received. Trichloroacetyl peroxide (TCAP) was prepared in situ by a known procedure.[9] Elemental analysis was performed by Schwarzkopf Lab.

The polymerizations of HFIB with VA were carried out under autogeneous pressure in glass tubes equipped with Teflon needle valves. Monomers were quantitatively introduced by vacuum transfer. The homogeneous polymerizations were carried out in bulk or in 1,1,3-trichlorotrifluoroethane solution at 30 and 0 °C. AIBN or Vazo-33 was used as initiator for polymerization at 30 °C while TCAP was used at 0 °C. The polymerization reaction was quenched by rapid cooling in liquid nitrogen. The polymer was collected and purified by precipitating it three times from a methylene chloride solution into methanol.

Copolymers of HFIB with vinyl alcohol (VOH) were obtained by hydrolysis of the HFIB–VA copolymer in THF solution under normal conditions (KOH, 60 °C/5 h). No residual acetoxy group was detected by NMR.

NMR experiments were carried out on a Varian XL-400 spectrometer, at frequencies of 400, 376.3, and 100 MHz for proton, fluorine, and carbon-13, respectively. DSC measurements were performed on a Du Pont 9900 instrument. X-ray diffraction patterns were obtained in the parafocus mode with Cu Kα radiation on a Philips diffractometer. Molecular weights were determined by light scattering in THF solution.

Results

Copolymer Composition. The electron deficiency of the HFIB double bond can be readily visualized from the ^{13}C NMR data of the monomer.[10,11] From the large chemical shift difference of the β-carbons of HFIB and VA (127.5 and 96.2 ppm, respectively), one may expect a preferred cross-propagation of these two monomers since the β-carbon chemical shift difference between comonomers has been suggested as a measure of alternation.[12–14] In the present copolymerization, as long as the mole fraction of VA in monomer load does not exceed 0.7, the resulted copolymer composition is always very close to 1:1. This is clearly shown in the monomer feed versus copolymer composition relationship of Figure 1 and Table

0024-9297/90/2223-0997$02.50/0

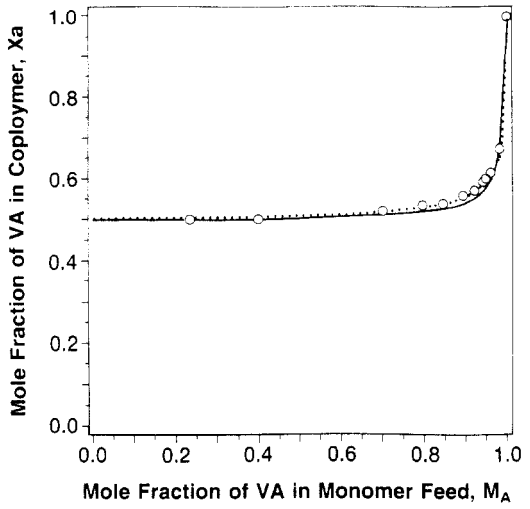

Figure 1. Copolymer composition vs monomer feed of the HFIB–VA system: M_A, mole fraction of VA in comonomer feed; X_a, mole fraction of VA in copolymer; point, experimental data; broken line, calculated from penultimate model with $r_{aa} = 0.0066$, $r_{ba} = 0.041$, and $r_{ab} = r_{bb} = 0$; solid line, calculated from the terminal model with $r_a = 0.021$.

I in which the copolymer compositions were obtained either from elemental analysis or by analysis of the proton NMR data.

Since the HFIB fraction in the copolymer for all monomer feed ratios does not exceed 0.5 and since the homopolymer of HFIB is not obtained under these conditions, it is reasonable to assume that the 1:1 copolymer is of alternating structure. We will therefore in the following treatment assume that HFIB is always present in the copolymer as a single unit sequence AB*A.

The 400-MHz proton NMR of a predominately 1:1 alternating copolymer is shown in Figure 2. Almost all monomer units (>95%) are arranged in head-to-tail structures. A small amount of block vinyl acetate is present in this sample as evident from the characteristic 5.1 ppm methine proton resonance. Other resonances from block vinyl acetate are obscured by the predominate alternate methylene and acetoxy methyl protons. The 5.1 ppm resonance is intensified in VA-rich copolymers. In the alternating VA–HFIB structure, the methine proton appears at 5.48 ppm.

Two sets of geminal methylene protons are centered at 2.20 and 2.35 ppm. From the observed splittings in the spectrum and from the simplification of the spectrum upon spin decoupling of the methine proton, we have determined that the low-field methylene proton has a vicinal coupling to the methine proton of 7 Hz while the high-field methylene proton is coupled to the methine proton with a coupling of 2 Hz. Spin simulation experiments also support this conclusion. The spectrum is also complicated by the effects of the nearby geminal CF_3 groups.

From the coupling constants, it can be established that the low-field methylene is trans to methine (H_t) and the high-field one is gauche (H_g); the g^+ configuration can be ruled out.

In the three possible conformers, tt, tg^-, and g^-g^-, formed by rotation around the C_α–C_β and C_α–$C_{\beta'}$ bonds in Structure 1, the g^-g^- conformer, is unlikely owing to steric hindrance of the CF_3's at the γ- and γ'-positions. The tg^- conformer can also be dismissed as this will induce unequality of the H_g's and H_t's on the β- and β'-carbons. We therefore conclude that the tt conformer is the most probable. This may imply that the copolymer molecule adopts a rigid and extended chain conformation in dilute solution and that rotation about the main chain C–C bonds is slow on the NMR time scale.

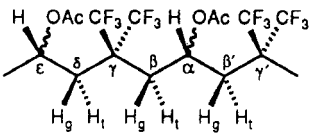

structure 1 (*ABABA*)

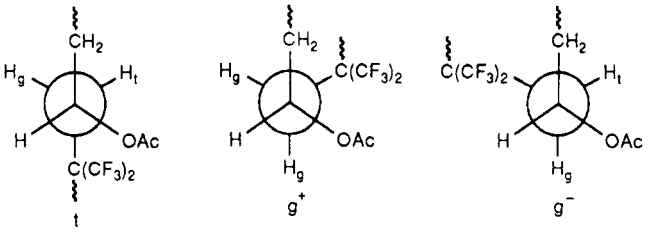

The methylene spectra also indicate the absence of the HFIB–HFIB sequences. Should these diads be present, there would be methylenes clamped between two $>C(CF_3)_2$ and we would therefore expect a chemical shift lower than is observed.

It is known in the NMR spectra of VA polymers that the methine part is most sensitive to its surroundings.[15] In the HFIB–VA copolymer, as the VA fraction increases, the spectra of the methine proton becomes more complicated and can be further divided into three subgroups. This is shown in Figure 3. The 5.3–5.5 ppm peak, as in the 1:1 alternating copolymer, is assigned to a VA unit centered in a HFIB–VA*–HFIB triad. The 4.8–5.0 peak is assigned to a VA centered in a VA–VA*–VA triad by consistency with those in VA homopolymers. Since substitution of one VA neighbor by HFIB induces a downfield shift, the 5.0–5.3 ppm peak is assigned as VA–VA*–HFIB triads. A close resemblance to this system is the vinyl acetate–vinylidene chloride case in which methine protons of the central VA in the VA–VA*–VA, VA–VA*–VDCl, and VDCl–VA*–VDCl triads are centered at 4.89, 5.43, and 5.89 ppm, respectively.[16]

The three methine subgroups from VA–VA*–VA, VA–VA*–HFIB, and HFIB–VA*–HFIB triads are well resolved in the 400-MHz spectra; the fractions of VA in these triads can be directly obtained from integration and the results are shown in Table I.

With the above assignments, it is possible to calculate the copolymer composition according to

$$X_a/X_b = 1 + (2F_{AAA} + F_{AAB+BAA})/(2F_{BAB} + F_{AAB+BAA}) \quad (1)$$

where X_a and X_b are the mole fractions of VA and HFIB in the copolymer, respectively, and F_{AAA}, $F_{AAB+BAA}$, and F_{BAB} are the relative intensities of the said triads. Since F_{BBB}, F_{ABB}, and F_{BBA} are all zero, the relative intensities are indeed unconditional probabilities. The copolymer compositions calculated from triad intensities are listed in Table I together with those obtained from elemental analysis. Differences between individuals in these two sets of data are smaller than 0.05, the estimated experimental error. The good agreement between the two sets of data lends support for the correctness of triad assignments and the validity of the composition data derived from NMR.

Monomer Reactivity Ratios. Two linear methods, the Fineman–Ross[17] and the Kelen–Tüdős[18] procedures, were used to determined the monomer reactivity ratios, but both of them failed to give a linear correlation. This is exemplified in Figure 4 by the bending of

Table I
Monomer and Copolymer Compositions, Conversions, and the Experimental Triad Fractions of the HFIB/VA Copolymerization[a]

sample	M_A in monomer feed, mole fractn[b]	conversn,[c] %	mol wt M_w, $\times 10^5$	X_a (copolymer compositn), mole fractn		VA-centered triad fraction[f]		
				a[d]	b[e]	F_{BAB}	$F_{(AAB+BAA)}$	F_{AAA}
1	0.9846	1.2	12.1	0.6830	0.678	0.145	0.658	0.197
2	0.9616	1.3	6.1	0.6203	0.620	0.294	0.635	0.072
3	0.9608	1.7	4.1	0.6047	0.606	0.350	0.602	0.049
4	0.9439	1.2	4.9	0.5970	0.596	0.393	0.571	0.036
5	0.9227	1.3	8.8	0.5731	0.575	0.500	0.477	0.023
6	0.8947	0.8	6.4	0.5588	0.562	0.566	0.425	0.009
7	0.8467	0.7	4.9	0.5389	0.541	0.658	0.342	*g*
8	0.7965	1.0	8.9	0.5312	0.537	0.726	0.274	*g*
9	0.7022	0.6	7.9	0.5109	0.523	0.825	0.175	*g*
10	0.3982	7.6	7.8	0.5028	0.508	0.938	0.063	*g*
11	0.2363	1.6	8.4	0.5051	0.504	0.971	0.029	*g*

[a] Bulk copolymerization of HFIB and VA at 30 °C, using 0.2% AIBN as initiator. [b] Mole fraction of VA in monomer feed. [c] Wt % of total monomer feed. [d] Mole fraction of VA in copolymer, calculated from elemental analysis. [e] Mole fraction of VA in copolymer, calculated from triad fractions. [f] Calculated from NMR areas of methine protons, $F_{AAA} = F_{(AAB+BAA)} = F_{BAB} = 1$. [g] Below NMR estimation level.

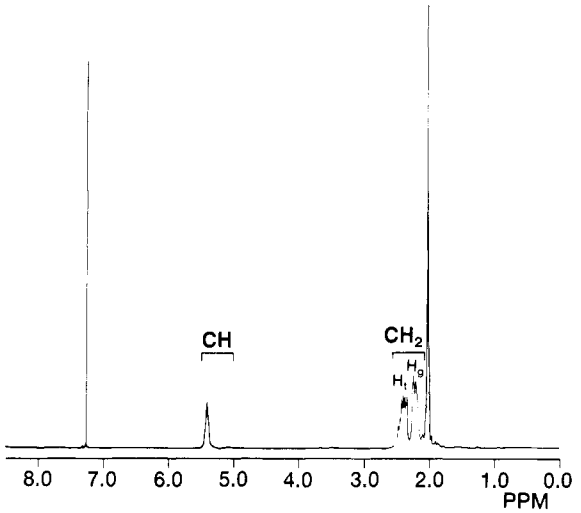

Figure 2. Proton NMR spectrum of an alternating VA–HFIB copolymer in $CDCl_3$ (sample 13 in Table V: mole fraction of VA in copolymer = 0.513, $M_w = 1.4 \times 10^6$).

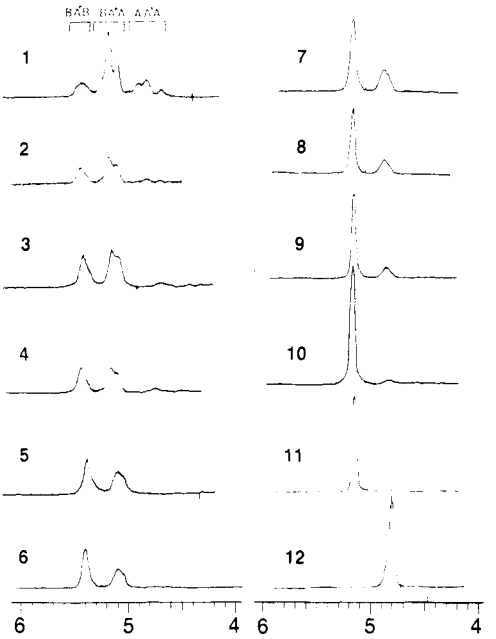

Figure 3. Subspectra of the methine protons of VA–HFIB copolymers. Sample number and mole fraction of VA in copolymers are as follows: 1, 0.683; 2, 0.620; 3, 0.605; 4, 0.597; 5, 0.573; 6, 0.559; 7, 0.539; 8, 0.531; 9, 0.511; 10, 0.503; 11, 0.505; 12, 0 (PVA).

the Kelen–Tüdós plot. The monomer feed ratios were selected so as to optimize the reactivity determination.[19] While at low VA concentrations a linear relationship that corresponds to $r_a = 0.3$ and $r_b = 0$ can be recognized, the curve deflects at high VA feed. In our experiment, the polymer conversion was maintained at a very low level compared to the amount of the minor comonomer. The accuracy of the monomer feed was controlled by careful weighing. The major error, therefore, would come from the polymer composition data for which we do not expect an increasing nonrandom deviation at higher VA ratios since two data sets obtained from two independent methods are consistent. Thus the deviations from linearity at high VA concentrations would be well outside our experimental error.

A nonlinear least-squares (NLLS) curve-fitting procedure for both the terminal and the penultimate models[20] was then applied to the experimental data. In both cases, convergence occurred after six to seven iterations of computation. For the penultimate model, calculations with restrictions (assuming r_{bb} or both r_{bb} and r_{ab} to be zero and search for the rest of the r's) gave the same results as those without restriction. The NLLS results are listed in Table II together with the calculated standard error S_x. The magnitude of S_x for the terminal model is considerably larger than that of the penultimate one, the latter being comparable with the experimental error. The polymer compositions calculated from the NLLS values of both models are compared with the experimental data, as shown in Figure 1. The penultimate curve fits more closely to the experimental data. As is evident in the literature,[21-24] the difference between the terminal and the penultimate model is most sensitively reflected in the sequence distributions. For this purpose we calculated the number fractions of VA sequences of length one to three from the two sets of NLLS r's and from the experimental triad concentrations by using the formulas listed in Table III.[25]

Figures 5–7 show the number fractions of VA sequences of length one, two, and three obtained from the experimental triad concentrations along with the predictions from the two models. In all three cases the penultimate model fits the experimental data significantly better than the terminal model.

Since sequence distribution is directly related to the reactivity ratios, as further evidence for the reality of the penultimate mechanism in VA–HFIB system we also calculated the monomer reactivity ratios directly from the experimental triad distributions.[22,23]

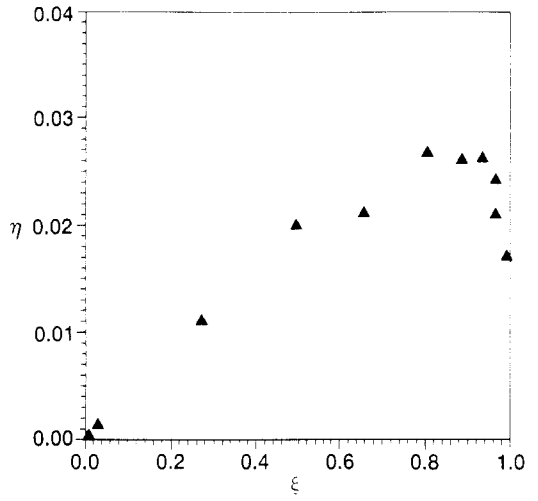

Figure 4. Kelen–Tüdós plot[18] of the HFIB–VA copolymerization.

Table II
Calculated Monomer Reactivity Ratios for the Copolymerization of HFIB with VA in Bulk at 30 °C

Penultimate Model

	NLLS[a]			seq distn[b]
	no restrictn	$r_{bb} = 0$	$r_{ab} = r_{bb} = 0$	$r_{ab} = r_{bb} = 0$
r_{aa}	0.00661	0.00662	0.00662	0.00724
r_{ba}	0.0405	0.0405	0.0405	0.0429
r_{bb}	0.0000	0.0000		c
r_{pb}	0.00010	c	c	c
S_x^d	0.00467	0.00437	0.00412	0.00513

Terminal Model

	NLLS[a]	seq distn[b] $r_b = 0$
r_a	0.0214	0.0347
r_p	0.000	c
S_x^d	0.0183	0.0383

[a] Calculated by nonlinear least-squares curve fitting.[20] [b] Calculated by sequence distribution (Scheme I). [c] Value fixed at zero. [d] Standard error $S_x = [\sum(X_c - X_e)^2/(n-d)]^{0.5}$, where X_c and X_e are the calculated and experimental VA mole fraction in copolymer, respectively, and n and d are the number of data points and variables in the model, respectively.

In our case since HFIB does not react with the HFIB radical, $k_{bb} = 0$ and $F_B = F_{AB} = F_{ABA}$, the reactivity ratios related to the HFIB radical are 0 and those related to the VA radical can be calculated according to Scheme I. From each experimental run in Table I, one set of r_a, r_{aa}, and r_{ba} could be obtained.

If the polymerization mechanism follows the terminal model, all r_a's obtained would be same and equal to r_{aa} and r_{ba}. However, if the penultimate model holds, then r_a is not constant and r_{aa} is different from r_{ba} although each of the latter two remain invariable. The calculated r_a, r_{aa}, and r_{ba} values are listed in Table IV. It is evident that the terminal model is not followed as r_a increases with increasing VA in the monomer feed; r_{ba} is about six times larger than r_{aa}, and both of them remain relatively stable at different monomer feed. The average r_{aa} and r_{ba} values are consistent with the NLLS results as shown in Table II.

From the above discussion we conclude that in the copolymerization of HFIB with VA, a penultimate model is preferred. To our knowledge, the HFIB–VA system is one of the very few cases in which the penultimate mechanism could be unambiguously established.

We postulate that the penultimate mechanism is best explained on steric grounds. The r_{aa} may represent the "real" reactivity difference of the two monomers toward a less hindered chain VA radical (–VA–VA•). For the –HFIB–VA• radical, the two bulky trifluoromethyl groups at the γ-position makes it significantly less reactive toward the bulky HFIB monomer.

Steric Configuration. The ^{19}F NMR spectrum of an alternating copolymer (sample 13 in Table V) is shown in Figure 8. There are three major peaks at –67.6 (peak c), –69.0 (peak d), and –69.8 (peak e) ppm with an area ratio of c:d:e = 1.01 ± 0.02:1.08 ± 0.02:1.00. Since a HFIB radical does not react with a HFIB monomer, every HFIB unit must therefore have VA units on either side. Thus the complexity observed in the ^{19}F NMR spectra must therefore stem from the steric configuration in VA–HFIB–VA sequences.

The VA–HFIB–VA triad or the HFIB–VA–HFIB–VA–HFIB pentad has two possible configurations, *m*(eso) or *r*(acemic):

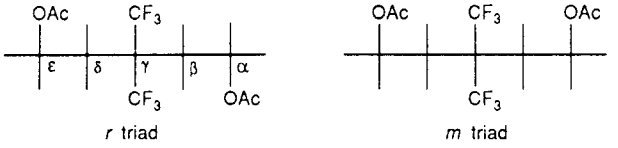

The fluorines of the two trifluoromethyls in the *r* configuration are equivalent. Those in the *m* configuration are not and appear in the ^{19}F NMR spectrum as two resonances of equal intensity. The ^{19}F resonance of the *r*-CF_3 which has one adjacent acetoxy group is predicted to be franked between those of the two unequivalent *m*-CF_3's having no or two adjacent acetoxys. Therefore peak d in Figure 8 corresponds to *r*-CF_3 and peaks c and e are related to the *m*-CF_3's. Support of the above assignment came from the ^{13}C NMR studies of alternating copolymers of vinyl acetate–vinylidene cyanide (VDCN)[26,27] and of styrene–methyl methacrylate.[28–30] In the VA–VDCN copolymer the three –C*N resonances at 115.2, 114.8, and 114.3 ppm are corresponding to the cyano carbons having no, one, and two nearby acetoxy groups, respectively. By analogy and assume shielding effect from a nearby acetoxy, the *m*-CF_3 with no adjacent acetoxy group may positioned at lowest field (peak c). However, the assignment between the two *m*-CF_3's is not clearly verified and does not interfere with the following treatment. Small resonances (–68.35 and –68.90 ppm and some overlapped with the major ^{19}F resonances) in Figure 8 are assigned to the HFIB–VA–HFIB*–VA–VA or VA–VA–HFIB*–VA–VA pentads. These resonances are intensified in VA-rich copolymers.

The fractions of *m*- and *r*-ABA triads, F_m and F_r, can be calculated from the relative intensities I_d and $(I_c + I_e)$ of peaks d, c, and e, respectively:

$$F_m = (I_c + I_e)/(I_d + I_c + I_e)$$
$$F_r = 1 - F_m \quad (2)$$

For a stereorandom polymer, $F_m = F_r = 0.5$. This has been proved to be true for most copolymers obtained under radical conditions such as alternating copolymers of vinylidene cyanide (VDCN)[26,27] and of styrene–methyl methacrylate.[28] It is interesting that in the present system populations of the *m*- and *r*-VA–HFIB–VA triads are not equal, suggesting a ε-position tacticity.[26] The tacticity of the copolymer is related to polymerization conditions, as shown in Table V. The stereoselectivity is increased at lower temperature, for the copolymers prepared at 0 °C, F_m and F_r are 0.65 ± 0.02 and 0.35 ± 0.02, respectively.

Table III
Fractions of VA Sequences

	from exptl triad concn	calcd from monomer reactivity ratios	
		terminal	penultimate
N_{BAB}[a]	$\frac{2F_{BAB}}{2F_{BAB} + F_{AAB+BAA}}$	$1 - P_{AA}$	$1 - P_{BAA}$
N_{BAAB}[a]	$\frac{F_{AAB+BAA}^2}{[2F_{BAB} + F_{AAB+BAA}][2F_{AAA} + F_{AAB+BAA}]}$	$P_{AA}(1 - P_{AA})$	$P_{BAA}(1 - P_{AAA})$
N_{BAAAB}[a]	$N_{BAAB}\frac{2F_{AAA}^2}{2F_{AAA} + F_{AAB+BAA}}$	$P_{AA}^2(1 - P_{AA})$	$P_{BAA}P_{AAA}(1 - P_{AAA})$
		$P_{AA} = \frac{M_A}{M_A + M_B/r_a}$	$P_{AAA} = \frac{M_A}{M_A + M_B/r_{aa}}$
			$P_{BAA} = \frac{M_A}{M_A + M_B/r_{ba}}$

[a] N_{BAB}, N_{BAAB}, and N_{BAAAB} are number fractions of VA sequences of length one, two, and three, respectively.

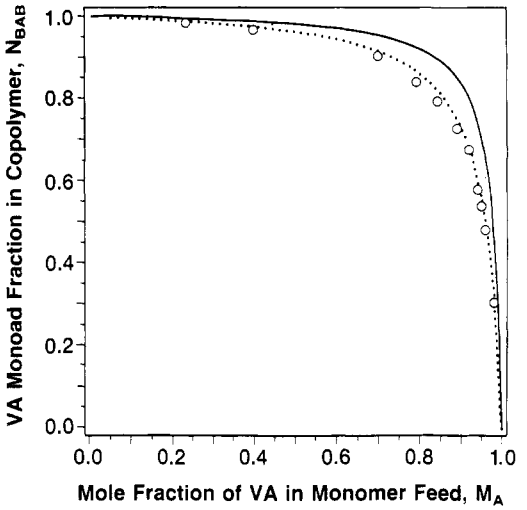

Figure 5. Fraction of VA unit sequences (BAB) as a function of mole fraction of VA in monomer feed: N_{BAB}, number fraction of VA sequence of unit length in copolymer; M_A, mole fraction of VA in monomer feed; points, experimental data; broken line, penultimate model; solid line, terminal model.

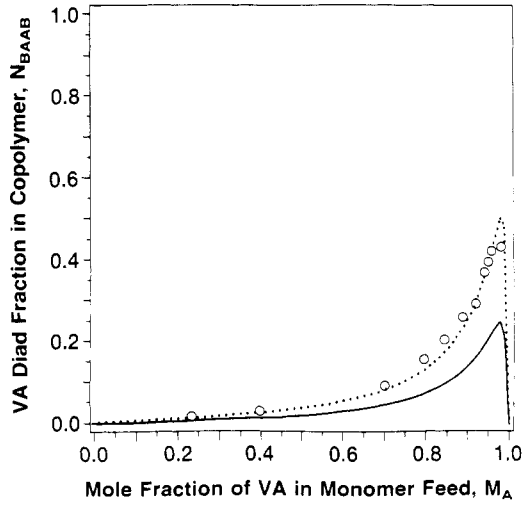

Figure 6. Fraction of VA diad sequences (BAAB) as a function of mole fraction of VA in monomer feed: N_{BAAB}, number fraction of VA sequences of length two in copolymer; M_A, mole fraction of VA in monomer feed; points, experimental data; broken line, penultimate model; solid line, terminal model.

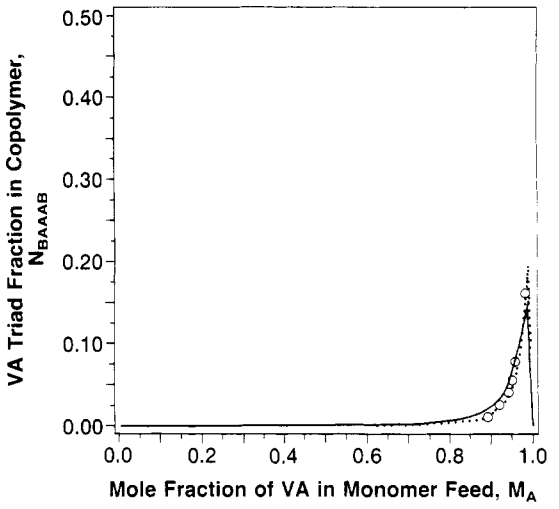

Figure 7. Fraction of VA triad (BAAAB) sequences as a function of mole fraction of VA in monomer feed: N_{BAAAB}, number fraction of VA sequences of length three in copolymer; M_A, mole fraction of VA in monomer feed; points, experimental data; broken line, penultimate model; solid line, terminal model.

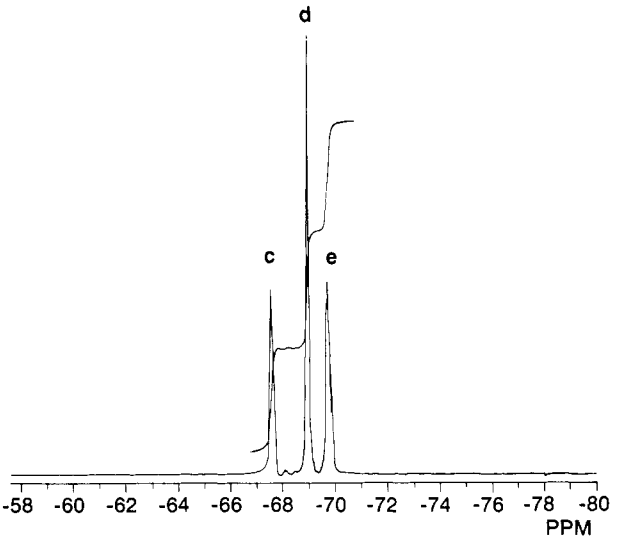

Figure 8. ^{19}F NMR spectrum of VA–HFIB alternating copolymer in $CDCl_3$ (sample 13 of Table V).

These results do not follow the established trend of stereoregularity in radical homopolymerization of vinyl monomers in which the *r* diad is generally favored and F_r increases with decreasing temperature.[31] The nature of the stereoselectivity in the current copolymerization is not clear.

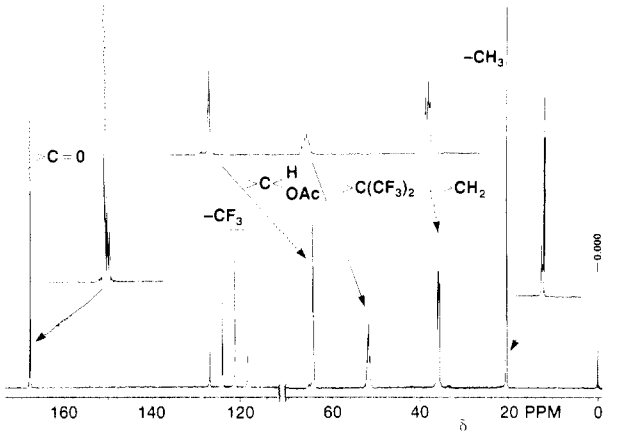

Figure 9. ^{13}C NMR spectrum of VA–HFIB alternating copolymer in $CDCl_3$ (sample 13 of Table V).

A test for the adequacy of the above stereochemical assignments from ^{19}F NMR is the fit of these results with the ^{13}C NMR data. The ^{13}C NMR spectrum of the same alternative copolymer is shown in Figure 9. All carbons except the trifluoromethyl carbon and the quaternary carbon at the γ-position in structure 1 appeared as multiple peaks due to tacticity. The trifluoromethyl carbon appears as a quartet with $^1J_{C-F}$ = 284 Hz. The γ-quaternary carbon bearing the two CF3 groups appears as two sets of partially overlapping septets with $^2J_{C-F}$ = 25 Hz. The remaining carbons did not exhibit obvious coupling to the CF_3 groups greater than the line widths.

The α-methine, acetoxy, methyl, and carbonyl carbon all appear as triplets. The methylene carbon appears as four resonances. Assignments, relative intensities, and comparison with calculated results are given in Table VI for all the carbons.

The splittings can be fully explained by configurational considerations. The two septets of the quaternary carbon are related to *m* and *r* triads.

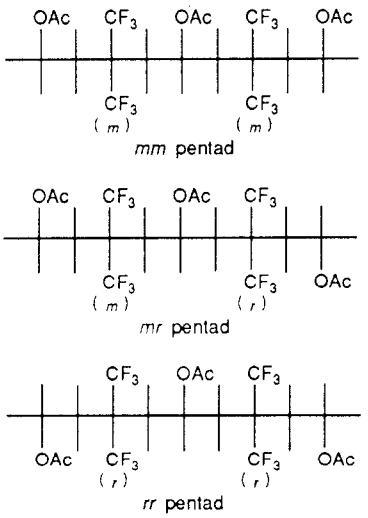

For all other carbons, a consideration of pentads is required. Three configurational pentads, *mm*, *mr*, and *rr*, are formed by connecting the *m* and *r* triads. Following Bovey's treatment[5] and assuming a Bernoullian process, fractions of these three pentads can be calculated from F_m and F_r:

$$F_{mm} = F_m^2$$
$$F_{mr} = 2F_mF_r \quad (3)$$
$$F_{rr} = F_r^2$$

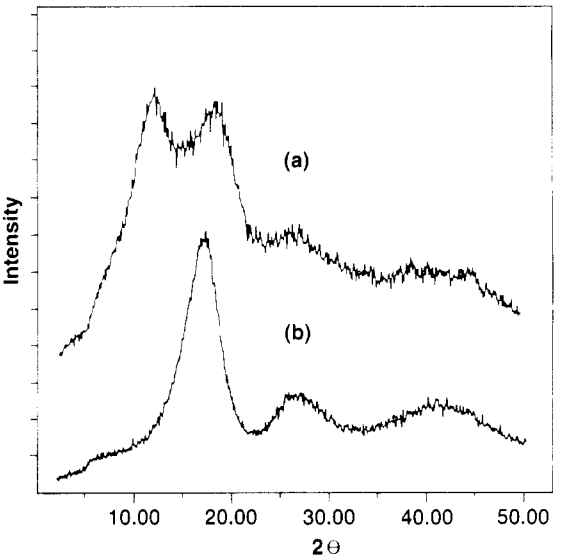

Figure 10. X-ray diffraction patterns of (a) HFIB–VA and (b) HFIB–VOH copolymers. Both samples were films of 0.1 mm. Diffraction angles and *d* spacings are as follows (2θ (deg), *d* spacing (Å)): for HFIB–VA copolymer, 6.71, 13.20; 11.53, 7.68; 17.90, 4.96; 26.44, 3.37; 40.96, 2.20; for HFIB–VOH copolymer, 6.26, 14.10; 16.63, 5.33; 26.16, 3.41; 40.96, 2.20.

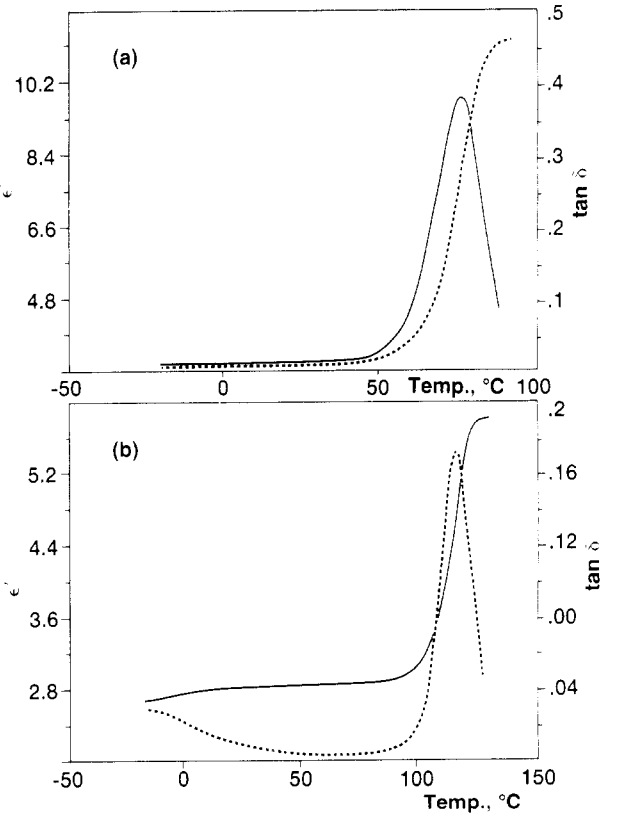

Figure 11. Dielectric relaxation of (a) HFIB–VA and (b) HFIB–VOH copolymer: dielectric constant ϵ' and dissipation factor (tan δ) vs temperature at 1000 Hz.

Using the F_m and F_r data from the ^{19}F NMR, fractions of these pentads can be calculated. As can be seen in Table VI, the calculated values are consistent with the measured results. The fact that all the ^{13}C splittings and their relative intensities can be explained on the basis of information obtained from ^{19}F NMR further documents the correctness of the stereochemical assignments.

Table IV
Monomer Reactivity Ratios Calculated According to Equations in Scheme I

sample	terminal model	penultimate model	
	r_a	r_{aa}	r_{ba}
1	0.0173	0.00734	0.0354
2	0.0250	0.00896	0.0427
3	0.0265	0.00803	0.0424
4	0.0280	0.00748	0.0431
5	0.0295	0.00804	0.0392
6	0.0334	0.00498	0.0442
7	0.0374		0.0471
8	0.0406		0.0482
9	0.0445		0.0450
10	0.0485		0.0503
11	0.0520		0.0489
average	0.0347 ± 0.0150	0.00724 ± 0.00124	0.0429 ± 0.0107

Scheme I
Calculation of Reactivity Ratios from Triad Distribution

Terminal Model

$$r_a = \frac{M_A(2F_{AAA} + F_{AAB+BAA})}{M_B(2F_{BAB} + F_{AAB+BAA})}$$

$$A^\bullet + VA \rightarrow A^\bullet \quad k_{aa}$$

$$A^\bullet + HFIB \rightarrow B^\bullet \quad k_{ab}$$

$$B^\bullet + VA \rightarrow A^\bullet \quad k_{ba}$$

$$B^\bullet + HFIB \rightarrow B^\bullet \quad k_{bb}$$

$$r_a = k_{aa}/k_{ab} \qquad r_b = k_{bb}/k_{ba} = 0$$

Penultimate Model

$$r_{aa} = \frac{M_B}{M_A}\frac{2F_{AAA}}{F_{AAB+BAA}}$$

$$r_{ba} = \frac{M_B}{M_A}\frac{F_{AAB+BAA}}{2F_{BAB}}$$

$$AA^\bullet + VA \rightarrow AA^\bullet \quad k_{aaa} \qquad AB^\bullet + VA \rightarrow BA^\bullet \quad k_{aba}$$

$$AA + HFIB \rightarrow AB^\bullet \quad k_{aab} \qquad AB^\bullet + HFIB \rightarrow BB^\bullet \quad k_{abb}$$

$$BA^\bullet + VA \rightarrow AA^\bullet \quad k_{baa} \qquad BB^\bullet + VA \rightarrow BA^\bullet \quad k_{bba}$$

$$BA^\bullet + HFIB \rightarrow AB^\bullet \quad k_{bab} \qquad BB^\bullet + HFIB \rightarrow BB^\bullet \quad k_{bbb}$$

$$r_{aa} = k_{aaa}/k_{aab} \qquad r_{ba} = k_{baa}/k_{bab}$$
$$r_{ab} = K_{abb}/k_{aba} = 0 \qquad r_{bb} = k_{bbb}/k_{bba} = 0$$

Properties. The acetoxy group in HFIB–VA copolymer can be hydrolyzed under normal alkaline conditions. The reaction was complete after stirring with excess KOH in THF solution at 50–60 °C for 5–8 h; no signals from residual acetoxy were detected by NMR. From a HFIB–VA copolymer of $M_w = 5.6 \times 10^5$ the resulting HFIB–VOH copolymer has a M_w of 4.8×10^5, indicating that no chain scission has occurred. The HFIB–VA copolymer can be dissolved in acetone and halogenated solvents; the HFIB–VOH copolymer dissolves in alcohol. Both copolymers can make transparent films by casting or molding. The HFIB–VOH films tend to craze upon folding.

The macroscopic structure of HFIB copolymers was examined by X-ray diffractions (XRD). XRD patterns of the HFIB–VA and HFIB–VOH copolymers are shown in Figure 10. Bulk and film samples are identical in XRD. Both copolymers are noncrystalline. The presence of multiple amorphous halos suggests that there might be some kind of order along the chain axis; however, annealing at 105 °C and stretching to 300–400% showed no difference in the XRD pattern. The most intense peak at a 2θ of 16.6° in HFIB–VOH copolymer is probably related to a large interchain separation of 5.3 Å, reflecting loose packing of the polymer molecules due to the bulky trifluoromethyls in HFIB. In the HFIB–VA copolymer there are two intense peaks at 2θ values of 11.5° and 17.9°, respectively; the reason for this is not clear at present.

The glass transition temperatures of the alternating HFIB–VA copolymer were measured by DSC and are reported in Table V. The molecular weight dependent T_g of the copolymer lies between 44 and 63 °C. Converting the acetoxy group into hydroxyl raised the T_g about 25 °C. In both copolymers no T_m was observed up to the decomposition temperature of 350 °C. Similar T_g ranges were observed from the dielectric measurements as shown in Figure 11, 55 and 95 °C for the HFIB–VA and the HFIB–VOH copolymers, respectively.

The alternating HFIB–vinylidene fluoride (VDF) copolymer was reported to have a T_g of 132 °C from dielectric and dynamic mechanical relaxation studies.[3] This value is extraordinary high for a symmetrically substituted copolymer and was explained by reasons of intrachain steric crowding. Severe steric crowding in the HFIB–VDF copolymer was also revealed by lack of calorimetrically observable T_g and the helix ttgg conformation in the crystalline lattice.[4]

For many copolymer systems the T_g of a copolymer is related to the T_g's of the two homopolymers and the copolymer composition.[32] Assuming that a simplified Gordon–Taylor relationship[33] (copolymer's T_g is an average of weight fractions of the two homopolymers) could be applied to the HFIB–VDF copolymer system, the T_g of the hypothetical HFIB homopolymer is predicted to be 197 °C.[3]

From the T_g's of PVA and of the hypothetical HFIB homopolymer (32 and 197 °C, respectively), T_g's of the present HFIB–VA and HFIB–VOH copolymers are predicted to be 142 and 175 °C, respectively, which are 80–100 °C higher than the experimental values. This inconsistency implies that the chain stiffening factor which drives the high T_g of the HFIB–VDF system is much less profound in the HFIB–VA and HFIB–VOH copolymers due to the flexible VA or VOH units. The significant T_g transition of these two copolymers observed in DSC also indicates that a certain degree of freedom is gained above the T_g. From the T_g's of the current two copolymer systems, it is predicted that the T_g of a hypo-

Table V
Effect of Reaction Condition on Stereoselectivity

sample	polym condn	fractn VA in monomer, M_A	$10^5 M_w$[a]	T_g, °C	fractn VA in polymer, X_a	fractn of *m* and *r* triad[b]	
						F_m	F_r
10	30 °C, bulk[c]	0.40	7.8	46	0.508	0.592	0.408
12	30 °C, soln[d]	0.40	6.7	44	0.508	0.609	0.391
13	0 °C, soln[e]	0.40	13.6	62	0.513	0.651	0.350

[a] Measured by light scattering in THF. [b] F_m and F_r are calculated from relative intensities of peaks c, d, and e in the ^{19}F NMR. [c] In bulk, use 0.2% AIBN as initiator. [d] In 20% 1,1,3-trichloro–trifluoroethane solution, use 0.2% Vazo-33 as initiator. [e] In 20% 1,1,3-trichloro–trifluoroethane solution, use 0.4% TCAP as initiator.

Table VI
Chemical Shift Values, Assignments, and Relative Intensities of the ^{13}C Signals[a]

species in alternate sequences	chem shift, ppm	tentative assignmt	rel intensities[b] expt	calcd
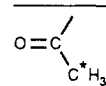	20.88	*rr*	0.13	0.12
	20.78	*mr*	0.49	0.46
	20.67	*mm*	0.38	0.42
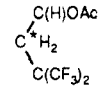	36.54	*rr*	0.08	0.12
	36.44	*mr* (or *rm*)	0.27	0.23
	36.11	*mm*	0.41	0.42
	35.93	*rm* (or *mr*)	0.22	0.23
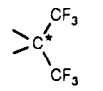	52.16[c]	*m*	0.62	0.65
	51.91[c]	*r*	0.38	0.35
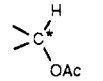	64.94	*mm*	0.29	0.42
	64.78	*mr*	0.52	0.46
	64.62	*rr*	0.19	0.12
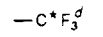	124.41 (J_{C-F} = 284 Hz)			
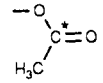	169.76	*mm*	0.40	0.42
	169.60	*mr*	0.48	0.46
	169.43	*rr*	0.12	0.12

[a] Data in this table are from sample 10 of Table I. [b] Intensities normalized over each species. [c] Center of septet, J_{C-F} = 25 Hz. [d] Insensitive to configuration, no further splitting other than C–F coupling.

thetical HFIB homopolymer with less steric crowding lies between 80 and 90 °C. This value may be useful in assessing the T_g's of copolymers from HFIB and other less-hindered monomers.

In summary, the copolymers of HFIB and VA were obtained under free radical conditions in bulk and in solution. The microstructure of the copolymers were studied by proton, carbon-13, and fluorine NMR. Consistent monomer reactivity ratios were obtained by a nonlinear least-squares procedure and by the sequence distributions. A penultimate mechanism is predominant with r_{aa} and 0.0066, r_{ba} = 0.041, and r_{bb} = r_{ab} = 0. Configurational studies indicated that the alternating copolymer has a certain degree of stereoregularity that is related to polymerization temperature. The alternating copolymers of HFIB and vinyl alcohol were also prepared. Bulk properties of copolymers were examined by DSC, dielectric relaxation, and XRD methods. Both copolymers are noncrystalline.

Acknowledgment. Helpful discussions and technical assistance from Drs. D. T. Hill, S. Chandrasekran, G. Stanitis, Y. Khanna, R. N. Majumdar, K. Zero, N. S. Murthy, and W. B. Hammond is gratefully acknowledged.

References and Notes

(1) Minhas, P. S.; Petruccelli, F. *Plast. Eng.* **1977**, *33*(3), 60.
(2) Hsu, S. L.; Sibilia, J. P.; O'Brien, K. P.; Snyder, R. G. *Macromolecules* **1978**, *11*, 990.
(3) Pochan, J. M.; Hinman, D. F.; Froix, M. F.; Davidson, T. *Macromolecules* **1977**, *10*, 113.
(4) Weinhold, S.; Litt, M. H.; Lando, J. B. *J. Polym. Sci., Polym. Phys. Ed.* **1982**, *20*, 535.
(5) Bovey, F. A.; Jelinski, L. W. *Chain Structure and Conformation of Macromolecules*; Academic: New York, 1982.
(6) Randall, J. C. *Polymer Sequence Determination*; Academic: New York, 1977.
(7) Modena, M.; Borsini, G.; Rogazzini, M. *Eur. Polym. J.* **1967**, *3*, 5.
(8) Gilbert, H.; Miller, F. F.; Averill, S. J.; Carlson, E. J.; Folt, V. L.; Heller, H. J.; Stewart, F. D.; Schmidt, R. F.; Trumbull, H. L. *J. Am. Chem. Soc.* **1956**, *78*, 1669.
(9) Zhao, C.; Zhou, R.; Pan, H.; Jin, X.; Qu, Y.; Wu, C.; Jiang, X. *J. Org. Chem.* **1982**, *47*, 2010.
(10) Loots, M. H.; Weinganlen, L. R.; Levin, R. H. *J. Am. Chem. Soc.* **1976**, *98*, 4571.
(11) Maciel, G. E. *J. Phys. Chem.* **1965**, *69*, 1947.
(12) Hatada, H.; Nagata, K.; Yuki, H. *Bull. Chem. Soc. Jpn.* **1970**, *43*, 3195, 3267.
(13) Herman, J. J.; Teyssié, P. *Macromolecules* **1978**, *11*, 839.
(14) Hatada, H.; Nagata, K.; Hasegawa, T.; Yuki, H. *Makromol. Chem.* **1977**, *178*, 2413.
(15) Ibrahim, B.; Katritzky, A. R.; Smith, A.; Weiss, D. E. *J. Chem. Soc., Perkin Trans. 2* **1974**, 1537.
(16) Johnson, U.; Kolbe, K. *Kolloid-Z. Z. Polym.* **1967**, *216/217*, 97.
(17) Fineman, M.; Ross, S. D. *J. Polym. Sci.* **1950**, *5*, 269.
(18) Kelen, T.; Tüdós, T. *J. Macromol. Sci., Chem.* **1965**, *A9*, 1.
(19) Tüdós, T.; Kelen, T. *J. Macromol. Sci., Chem.* **1981**, *A16*, 1283.
(20) Cais, R. E.; Farmer, R. G.; Hill, D. J. T.; O'Donnell, J. H. *Macromolecules* **1979**, *12*, 835. We thank Dr. Hill for sending us an IBM-PC version of this NLLS program.
(21) Fukuda, T.; Ma, Y. D.; Inagaki, H. *Polym. J.* **1982**, *14*, 705.
(22) Ito, K.; Yamashita, Y. *J. Polym. Sci.* **1965**, *A3*, 2165.
(23) Hill, D. T. T.; O'Donnell, J. H.; O'Sullivan, P. W. *Macromolecules* **1985**, *18*, 9.
(24) Tirrell, D. A. In *Encyclopedia of Polymer Science and Technology*, 2nd ed.; Wiley-Interscience: New York, 1986; Vol. 4, p 206.
(25) Hill, D. J. T.; O'Donnell, J. H.; O'Sullivan, P. W. *Macromolecules* **1982**, *15*, 960.
(26) Jo, Y. S.; Inoue, Y.; Chûjô, R.; Saito, K.; Miyata, S. *Macromolecules* **1985**, *18*, 1850.
(27) Inoue, Y.; Kashiwazaki, A.; Maruyama, Y.; Jo, Y. S.; Chûjô, R.; Seo, I.; Kishimoto, M. *Polymer* **1988**, *29*, 144.
(28) Heffner, S. A.; Bovey, F. A.; Verge, L. A.; Mirau, P. A.; Tonelli, A. E. *Macromolecules* **1986**, *17*, 1628.
(29) Hirai, H.; Koinuma, H.; Tanabe, T.; Takeuchi, K. *J. Polym. Sci., Polym. Chem. Ed.* **1979**, *17*, 1339.
(30) Niknam, M. K.; Majumdar, R. N.; Blouin, F. A.; Harwood, H. J. *Makromol. Chem., Rapid Commun.* **1982**, *3*, 825.
(31) Pino, P.; Suter, U. W. *Polymer* **1976**, *17*, 1977.
(32) Mark, J. E.; Eisenberg, A.; Graessley, W. W.; Mandelkern, L.; Koenig, J. L. *Physical Properties of Polymers*; American Chemical Society: Washington, DC, 1984.
(33) Wood, L. A. *J. Polym. Sci.* **1958**, *28*, 319.

Registry No. (HF1B)(VA) (alternating copolymer), 124286-62-0; HF1B, 382-10-5; VA, 108-05-4; (HF1B)(VOH) (alternating copolymer), 124286-63-1.